Volume Title
ASP Conference Series, Vol. **Volume Number**
Author
© **Copyright Year** Astronomical Society of the Pacific

Mode Frequencies from GONG, MDI, and HMI Data

S. G.Korzennik

Harvard-Smithsonian Center for Astrophysics, Cambridge, MA, USA

Abstract. I present recent results from fitting all the available data from the three major helioseismic instruments: GONG, MDI and HMI using my independent methodology. This method not only fits individual singlets, but: fits them simultaneously for a given multiplet; uses an optimal multi-taper spectral estimator; includes the full leakage matrix and the effect of mode distortion by differential rotation; and fits an asymmetric mode profile. The mode fitting was carried out on time series of varying lengths (1×, 2×, 4×, 8×, 16×, 32×, 64× 72 days long), using co-eval epochs for all three instruments. By fitting time series of varying lengths, one trades off some temporal resolution for a better precision. I present these results, compare them and discuss the potential sources of the discrepancies.

1. Introduction

I have fitted all the available data sets from the three major helioseismic instruments: GONG, MDI, and HMI. These data were analyzed with the same independent fitting procedure I developed a few years ago (see Korzennik 2005, 2008a,b). The data sets consist of 16.85 years of GONG observations (or 171 × 36 day-long segments), 14.98 years of MDI observations (or 76×72 day-long segments, with 2×72 day-long segments missing, namely the *whole* mission), and 1.97 years of HMI observations (or 10 × 72 day-long segments, with 5 × 72 day-long segments that overlap with GONG & MDI). The data were reduced to spherical harmonic coefficients by the respective projects. I used the MDI coefficients re-computed with an improved[1] spatial decomposition, while the HMI coefficients I used were still preliminary. The fitting methodology I used is described in detail in Korzennik (2005). Some of the salient points of the methodology worth mentioning here are as follow: (a) the method fits individual singlets (n, ℓ, m); (b) it uses an optimal sine-multitaper spectral estimator; (c) it takes into account the complete leakage matrix; and (d) it fits an asymmetric profile. To trade off precision and temporal resolution, time series of different lengths were fitted, namely not only 1×72 day long time series, but also 2×, 4×, 8×, 16×, 32×, 64×72 day long time series.

[1]The MDI project applied a spatial decomposition that included not only the instantaneous plate scale, but our best model of the instrumental image distortion.

2. Results

One important difference between the results of my fitting method and the respective project methods is mode attrition, namely, how often the same mode is successfully fitted for each epoch. The resulting mode attrition is shown in Figure 1. That figure illustrates how drastically different the attrition pattern is for each fitting methodology. There are at least two reasons why the attrition is important. First, for long enough time series (which should be the case for 72 and 108 day long time series), all the modes are expected to be excited with similar amplitudes for each epoch and thus the same set of modes should be successfully fitted each time. The fact that this is not the case suggests either that the length of the time series is not long enough, or that the fitting methodology is not optimal. Secondly, if we wish to extract from the data indicators of subtle changes in the Sun, we ought to analyze (e.g., invert) the same set of modes for each epoch. With a large attrition rate, the set of modes that is successfully fitted at each epoch over a full solar cycle is, in some cases, barely 10% of the fitted mode set.

A direct comparison between frequencies resulting from fitting GONG and MDI augmented by HMI data, using my method, is shown in Figure 2, in relative terms ($\delta\nu/\sigma_\nu$). These scaled differences are at the 2σ level, with a streak at low values of ν/L. That streak disappears when using longer time series. The figure also shows an enhanced difference, also limited to low ν/L, that dominates for the longer time series and is limited in time to epochs prior to the upgrade of the GONG camera. A similar comparison (not shown), but for the 5 epochs of co-eval data between MDI and HMI, shows discrepancies at the 2σ level, with a uniform distribution with respect to time and ν/L.

Figure 3 shows the relative frequency changes, now with respect to the first epoch, resulting from fitting either GONG or MDI observations (augmented by HMI observations), using my methodology, and epochs of increasing lengths. The figure indicates that using longer time series produces more significant changes, but at the cost of reduced temporal resolution. It also shows that the two data sets produce very similar, although not identical, results.

Figure 4 compares the mean frequency change with epoch, using MDI observations but different fitting methodologies. Two of the four sets were computed using tables resulting from fitting carried out by the MDI project, using either a symmetric or asymmetric profile. The other two sets were computed using the results of my fitting method, also using either a symmetric or asymmetric profile[2]. The resulting mean changes are compared to three solar activity indices. The magnitude of the mean changes corresponding to results of my fitting, using an asymmetric profile is substantially smaller than the ones resulting from the MDI project fitting results. The figure also shows that fitting an asymmetric profile reduces the the magnitude of the mean changes, compared to fitting a symmetric profile using the same fitting method for either methodology. Not surprisingly, the correlation of these changes with respect to any of the three solar indices is different.

The source of this discrepancy is to be found in the differences of the resulting fitted line widths and more importantly in the differences of the asymmetries. Figure 5 shows the variation of the FWHM and of the asymmetry, estimated by my fitting

[2]I also fitted all the 72-day long MDI time series with my methodology, modified to keep the asymmetry null.

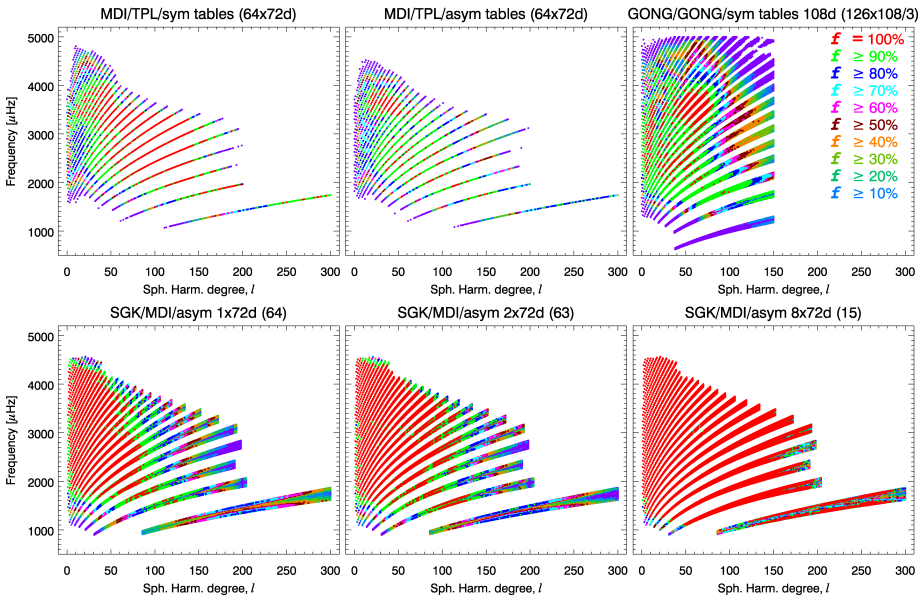

Figure 1. Fitting attrition rate, i.e., the fraction of time a given mode is fitted over some 13.6 years of observations (64×72-day long epochs). The top row shows the rates for tables produced by the respective projects, from left to right: MDI symmetric fit, MDI asymmetric fit, and GONG symmetric fit. The MDI fitting produced tables of multiplets, since that fitting uses a polynomial expansion in m to parametrize the singlets. The GONG fitting produced tables of singlets, fitting 126 epochs over that 13.6 year span, each 108-day long and offset by 36 days. The bottom row shows those rates for tables produced by my fitting using MDI data, with from left to right: fitting 64 epochs, each 72 day long, 63 epochs each 2×72-day long and offset by 72 days, and 15 epochs each 8×72-day long and offset by 4×72 days. Keep in mind that my fitting produces singlets, fitting all m values simultaneously, and uses an asymmetric profile.

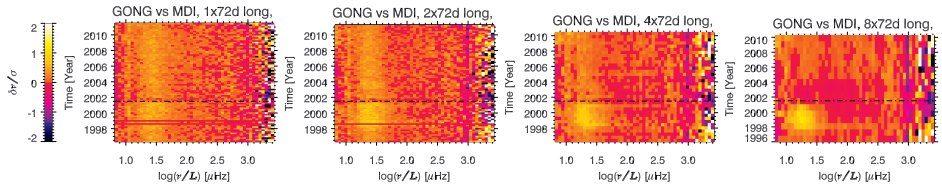

Figure 2. Comparison between fitted frequencies, scaled by their respective uncertainties, using my method on either MDI or GONG data, binned as a function of ν/L, and resulting from fitting 1×, 2×, 4×, 8×72-day long time series (left to right). A horizontal line is drawn around the time when the GONG camera was upgraded.

methodology (asymmetric fit), as a function of epoch. That figure shows a clear correlation of these changes with solar activity. It also shows a distinct dependence with

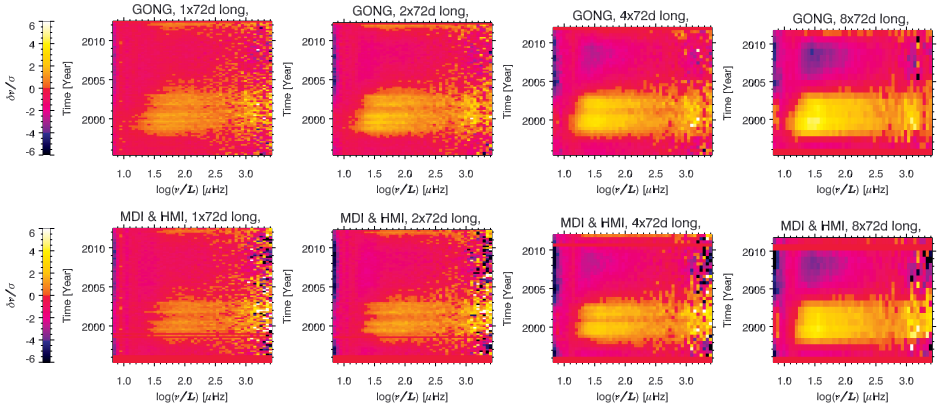

Figure 3. Relative frequency changes, $\delta\nu/\sigma_\nu$, with respect to the first epoch, for results of my fitting to either GONG (top row) or MDI augmented with HMI (bottom row) observations and for fitting epochs of different lengths (1×, 2×, 4×, 8 × 72-day long time series, from left to right).

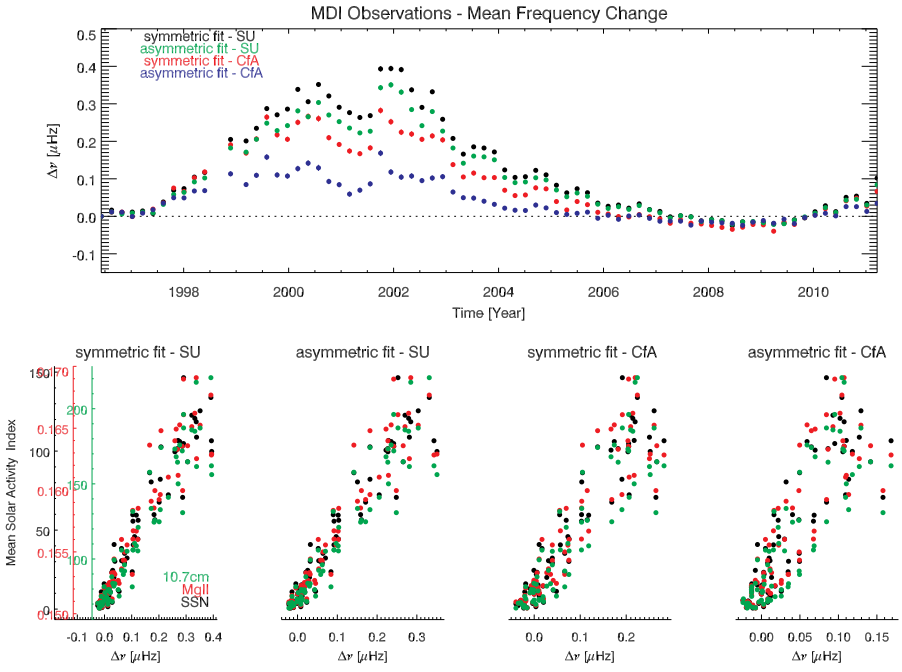

Figure 4. Top panel: mean frequency change with respect to epoch, when fitting MDI observations using symmetric or asymmetric fits, produced by the MDI project (SU) or by my own independent fitting (CfA). Bottom panels: the mean changes compared to three solar activity indices (sunspot number, Mg II core-to-wing index and the 10.7 cm radio flux). Left to right: symmetric/SU, asymmetric/SU, symmetric/CfA, asymmetric/CfA.

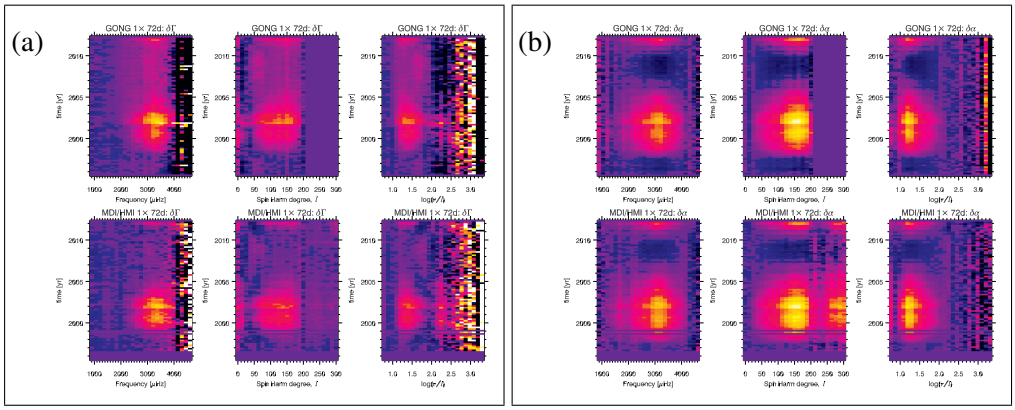

Figure 5. Change in FWHM (a) and asymmetry (b), as a function of ν, ℓ, or $\log(\nu/L)$ (left to right) and epoch –hence solar activity– resulting from using my fitting methodology. The top row shows results from fitting GONG observations, the bottom row from fitting MDI observations.

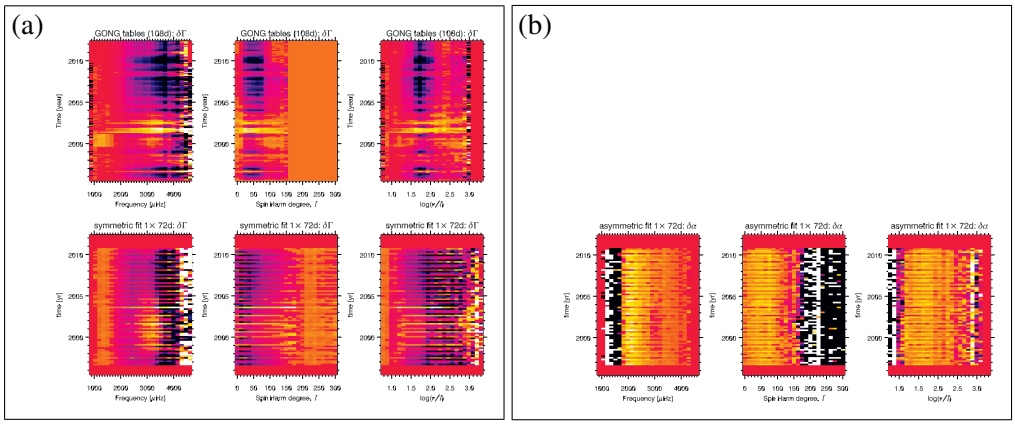

Figure 6. Change in FWHM (a) and asymmetry (b), as a function of ν, ℓ, or $\log(\nu/L)$ (left to right) and epoch, as in Fig. 5, but using the respective projects tables: GONG and MDI (top and bottom).

respect to frequency and spherical harmonic degree. Since my fitting reveals changes in asymmetries, it will affect the resulting changes in frequencies.

In contrast, Fig. 6 shows the measured change in FWHM and asymmetry seen in the respective project fitting tables. These changes are a lot more noisy, with substantial short term variations. Nevertheless, upon close scrutiny, one can detect a hint of correlation with solar activity. Indeed, the change of FWHM as estimated by the GONG project exhibits some increase at the peak of solar activity, although variations at low activity and at short periods are also present. Similarly, the change of FWHM as estimated by the MDI project, while also showing variations at all levels of activity with short periods, is also suggestive of an increase at times of high activity.

3. Conclusions

Analyzing GONG, MDI and HMI observations using the same fitting technique leads to comparable results, at the 2σ level. While this is not a significant difference, I find it surprisingly larger than anticipated. Comparison of co-eval data analyzed with the same techniques ought to produce results that are very similar. Differences at the 2σ level are suggestive of residual systematic errors, although not significant. The comparison between GONG and MDI shows systematic differences, with larger differences confined to a specific range of ν/L, except for the more accurate results using longer time series where the difference is primarily for epochs prior to the upgrade of the GONG camera.

The comparison of my fitting results to those produced by the respective projects shows that the frequency changes with activity are different. The reduction of the mean frequency change, when using my estimates, is the result of an observed change of the asymmetry (and to some level of the FWHM). Both the asymmetry and the FWHM measured using my fitting methodology show a clear variation that strongly correlates with solar activity levels and is confined to a ν/L range. Hints of a similar variation can be seen when looking closely at the estimates of the respective projects.

The variation of the FWHM and the asymmetry with activity suggests that the location of the mode excitation changes slightly as the Sun gets more active. The increase in activity results in larger FWHM, or shorter mode lifetime, and larger asymmetries. These changes are confined to a ν/L band, or to modes that penetrate down to similar depths. Closer inspection indicates that the peak of the FWHM changes might be located at a slightly different value of ν/L (or depth) than the peak of the change in asymmetry. The change in asymmetry with respect to the mode spherical harmonic degree shows a bi-modal distribution that we cannot readily explain, although results above $\ell = 200$ are restricted to f-modes (and to MDI observations).

Also, the resulting mean change of frequency, when taking into account the change of asymmetry, no longer shows a simple correlation with the solar activity indices. Instead, some level of hysteresis seems to be present.

Acknowledgments. The Solar Oscillations Investigation - Michelson Doppler Imager project on SOHO is supported by NASA grant NNX09AI90G at Stanford University. SOHO is a project of international cooperation between ESA and NASA. This work utilizes data obtained by the Global Oscillation Network Group (GONG) program, managed by the National Solar Observatory, which is operated by AURA, Inc. under a cooperative agreement with the National Science Foundation. The data were acquired by instruments operated by the Big Bear Solar Observatory, High Altitude Observatory, Learmonth Solar Observatory, Udaipur Solar Observatory, Instituto de Astrofísica de Canarias, and Cerro Tololo Interamerican Observatory. HMI data courtesy of NASA and the HMI consortium; HMI is supported by NASA contract NAS5–02139 to Stanford University. SGK was supported by NASA grants NAG5–9819 and NNG05GD58G ans NSF grant AGS–1037834.

References

Korzennik, S. G. 2005, ApJ, 626, 585
— 2008a, Astronomische Nachrichten, 329, 453
— 2008b, Journal of Physics Conference Series, 118, 012082